Supplementary Material

Flexible and conductive MXene/Silver nanowire films for enhanced detection and elimination of bacteria

Zixuan Jia [a,b], Huimin Miao [a,b], Mingna Hu [a,b], Jie Wu [b], Jiahui Cai [a,b], Xinlu Li [a,b], Zhimin Chang [a,b], Panyong Wang [a,b*], Li Li [a,b], Wen-Fei Dong [a,b*], Qiannan You [a,b,c*]

a School of Biomedical Engineering (Suzhou), Division of Life Sciences and Medicine, University of Science and Technology of China, Hefei 230026, P. R. China

b Department of Biomaterials and Stem Cells, Suzhou Institute of Biomedical Engineering and Technology, Chinese Academy of Science, Suzhou 215163, P. R. China

c Jinan Guoke Medical Technology Development Co., Ltd, Jinan 250103, P. R. China

Corresponding Author

[*] E-mail: wangpy@sibet.ac.cn; wenfeidong@sibet.ac.cn; youqn@sibet.ac.cn

S1. Materials

Ti_3AlC_2 powder (99%, 200 mesh) was purchased from 11 Technology Co., Ltd. (Jilin, China). Lithium fluoride (LiF) was purchased from Aladdin Biochemical Technology Co., Ltd. (Shanghai, China). Hydrochloric acid (HCl) was purchased from Lingfeng Chemical Reagent Co., Ltd. (Shanghai, China). Carbon cloth (CC) was purchased from Shengrnuo Technology Co., Ltd. (Suzhou, China). The aptamer of *S. aureus* (5'-SH-GCAATGGTACGGTACTTCCTCGGCACGTTCTCAGTAGCGCTCG CTGGGTCATCCCACAGCTACGTCAAAAGTGCACGCTACTTTGCTAA-3') was provided by Sangyo Bioengineering Co., Ltd. (Shanghai, China). Polyvinylpyrrolidone (PVP), ethylene glycol (EG), and potassium ferricyanide were purchased from Adamas Reagent Co., Ltd. (Shanghai, China). Silver nitrate, acetone, anhydrous ethanol, and PBS buffer were purchased from Sigma-Aldrich (USA). Sodium chloride was purchased from Sinopharm Chemical Reagent Co., Ltd. (Shanghai, China). Potassium dihydrogen phosphate and potassium chloride were purchased from Aladdin Biochemical Technology Co., Ltd. (Shanghai, China). Dipotassium hydrogen phosphate, potassium ferricyanide, LB-liquid medium, and LB-solid medium were purchased from Titan Technology Co., Ltd. (Shanghai, China). *Escherichia coli* (ATCC 25922) and *Staphylococcus aureus* (ATCC 29213) were purchased from Beijing Microbial Strain Preservation Center. *Pseudomonas aeruginosa* (ATCC 27853) and *Enterococcus faecalis* (ATCC 29212) were obtained from Luwei Technology Co., Ltd. (Shanghai, China). Bacillus subtilis (BNCC 109047) was purchased from Beina Biotechnology Co., Ltd. (Hebei, China). Fetal bovine serum and trypsin were purchased from Gibico (USA). The WST-1 cell proliferation and cytotoxicity assay kit was purchased from Tianyu Biotechnology Co., Ltd. (Shanghai, China). All chemicals were of analytical reagent grade or better, and all aqueous solutions were prepared with deionized water.

S2. Apparatus

Scanning electron microscope (SEM) images were obtained on a Regulus-8100 instrument (Hitachi, Tokyo, Japan). Transmission electron microscopy (TEM) images

were obtained on an HT-7800 instrument (Hitachi, Tokyo, Japan). Ultraviolet absorption spectroscopy (UV-vis) was performed on a U-3900H spectrophotometer (Hitachi, Tokyo, Japan). X-ray diffraction (XRD) maps were characterized by D8 Advance (Bruker, MA, USA). X-ray photoelectron spectroscopy (XPS) was carried out on an AXIS ULTRA DLD (Shimadzu, Kyoto, Japan). Fourier transform infrared spectroscopy (FT-IR) was obtained on an IS50 (Thermo Fisher, MA, USA). Zeta potential measurements were performed with a Nano ZS/ZEN3690 instrument (Malvern, UK). Stained images of bacteria were captured using a Nikon A1R HD25 confocal microscope (Nikon, Tokyo, Japan).

S3. Electrochemical measurements

All electrochemical testing experiments were performed on a CHI 660E electrochemical workstation (Shanghai Chenhua Instrument Co., Ltd., China) with a three-electrode system (working electrode, saturated silver chloride (Ag/AgCl) reference electrode, and platinum wire counter electrode). The electrochemical testing methods and conditions used were: cyclic voltammetry (CV) was performed in an electrolyte containing 0.1 M KCl and 10 mM $K_3[Fe(CN)_6]$ to obtain redox curves of CC, CM, and CMA. The scan rate varied from 50 mV/s to 300 mV/s, with a scanning range of 0.2 to 0.6 V; differential pulse voltammetry (DPV) was employed to assess the electrochemical performance and bacterial capture efficacy of the biosensors. The scanning range was 0.2 to 0.6 V, using the same electrolyte as in cyclic voltammetry; the electrochemical impedance spectroscopy (EIS) test was performed by using 5 mM $[Fe(CN)_6]^{3-/4-}$ as the electrochemical probe and the frequency range was set to 0.1 Hz~100 kHz with the amplitude of 5 mV; and the chronoamperometric method (i-t) was performed by using a potential set to 0.2 V and the run time was 1000s.

S4. Cytotoxicity

To evaluate the cytotoxicity of the proposed system, the WST-1 Cell Proliferation and Cytotoxicity Assay Kit was used. Human lung cancer cells (NCI-A549) cells were cultured in DMED medium containing 10% fetal bovine serum and 100 U/mL penicillin-streptomycin solution in an atmosphere with 5% CO_2 at 37 ℃. The NCI-A549 cells were collected as cells supernatant when they were grown to

more than 80% and collected by centrifugation. The supernatant (100 μL, 1.0×10^4 cells/mL) was inoculated into 96-well plates and incubated in a thermostatic incubator (37°C, 5% CO_2) for 24 h. Then, different concentrations of MXene/AgNWs mixture were treated for 15 min and 18 hours, respectively. The wells with only medium added were used as a blank group, and in each well, 10 μL of WST-1 and 90 μL of culture medium were added and incubated, after 40 min, the absorbance of the samples was measured at 450 nm with an enzyme meter. Cell viability can be calculated by the following formula:

Cell viability = OD450 (sample) - OD450 (blank) / OD450 (control) - OD450 (blank) x 100%

S5. MXene/AgNWs synergistic antimicrobial mechanism

In order to investigate the mechanism of synergistic antimicrobial activity of MXene/AgNWs, the Ag^+ concentrations of AgNWs and MXene/AgNWs were measured over time. The standard curve of Ag^+ was obtained by measuring the absorbance of a standard concentration of $AgNO_3$ solution with NaCl to produce AgCl. The Ag^+ concentration of AgNWs and MXene/AgNWs at 0, 4, 8, 12 and 24 h were measured to obtain the relationship between MXene and Ag^+ release.

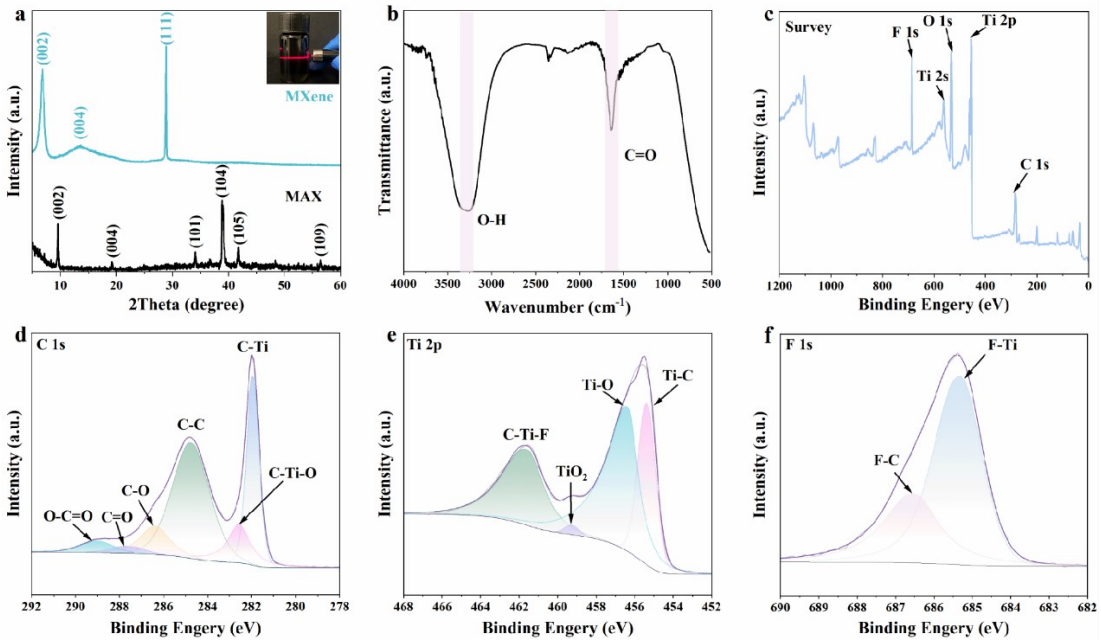

Fig. S1. (a) XRD patterns of Ti_3AlC_2 MAX and $Ti_3C_2T_x$ MXene (Silicon wafer as substrate); (b) FT-IR spectrum of $Ti_3C_2T_x$ MXene; XPS spectra of $Ti_3C_2T_x$ MXene: (c) survey spectrum, (d) C 1s, (e) Ti 2p, and (f) F 1s. As shown in Fig. S1b, the FT-IR spectrum showed two peaks at 3410 cm^{-1} and 1610 cm^{-1}, corresponding to -OH and C=O of $Ti_3C_2T_x$, respectively. In addition, the XPS energy spectrum of $Ti_3C_2T_x$ showed that the contents of C, O, Ti, and F were 13.25%, 24.32%, 47.05%, and 15.39%, respectively (Fig. S1c). The C1s region (Fig. S1d) shows that it is mainly composed of C-Ti (281.9 eV), C-Ti-O (282.6 eV), C-C (284.8 eV), C-O (286.4 eV), C=O (287.7 eV), and O-C=O (289.1 eV). The Ti 2p spectra (Fig. S1e) showed three peaks at 461.7 eV, 459.3 eV, 456.4 eV, and 455.4 eV, respectively, attributed to the C-Ti-F, TiO_2, Ti-O, and Ti-C bonds, which formed the internal lamellar structure of the two-dimensional MXene nanosheets. The F1s region (Fig. S1f) shows that it mainly consists of F-C (686.5 eV), and F-Ti (685.3 eV).

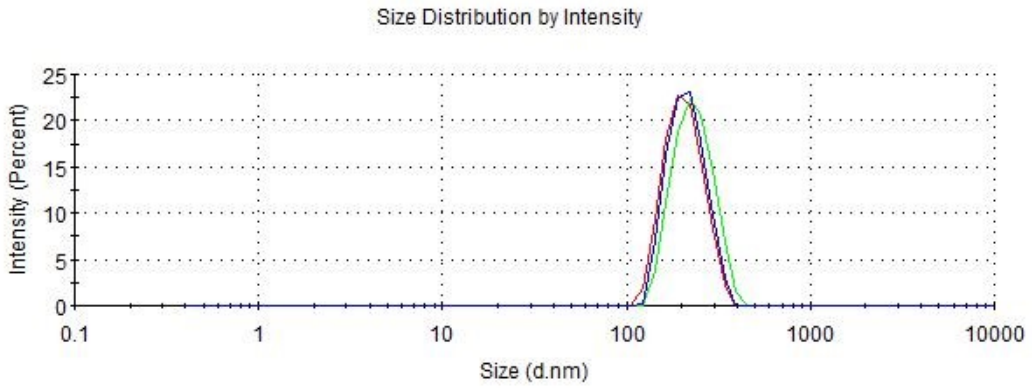

Fig. S2. Dynamic light scattering (DLS) of the $Ti_3C_2T_x$ MXene nanosheets. Three parallel characterizations were performed to determine the uniformity of MXene nanosheets synthesized in different batches under the same conditions. The mean nanosheet size of the as-prepared $Ti_3C_2T_x$ MXene can be calculated according to the formula of $a_{DLS} = 5.9 \times \ < L >^{0.66}$, where a_{DLS} is the peak value in the intensity particle size distribution curve, and $< L >$ represents the average size of the nanosheet. The peak value in Fig. S3 is around 171.7 nm, thus $< L >$ can be calculated to be 165.2 nm, showing that the average size of as-prepared $Ti_3C_2T_x$ MXene nanosheets is approximately 200 nm.

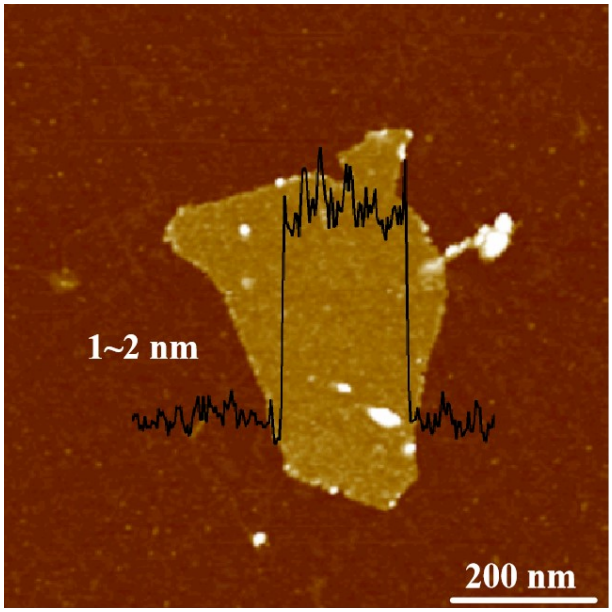

Fig. S3. AFM image of $Ti_3C_2T_x$ MXene nanosheets. As shown in Fig. S2, the height of the nanosheets was 1~2 nm, indicating the successful synthesis of single or double layers of MXene.

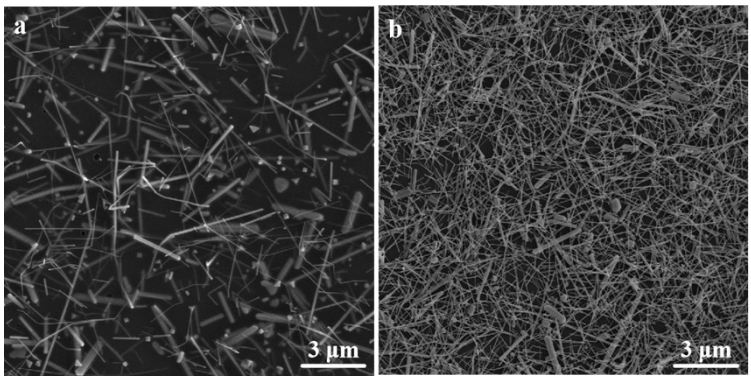

Fig. S4. SEM images of AgNWs reacting for (a) 240 min; (b) 80 min.

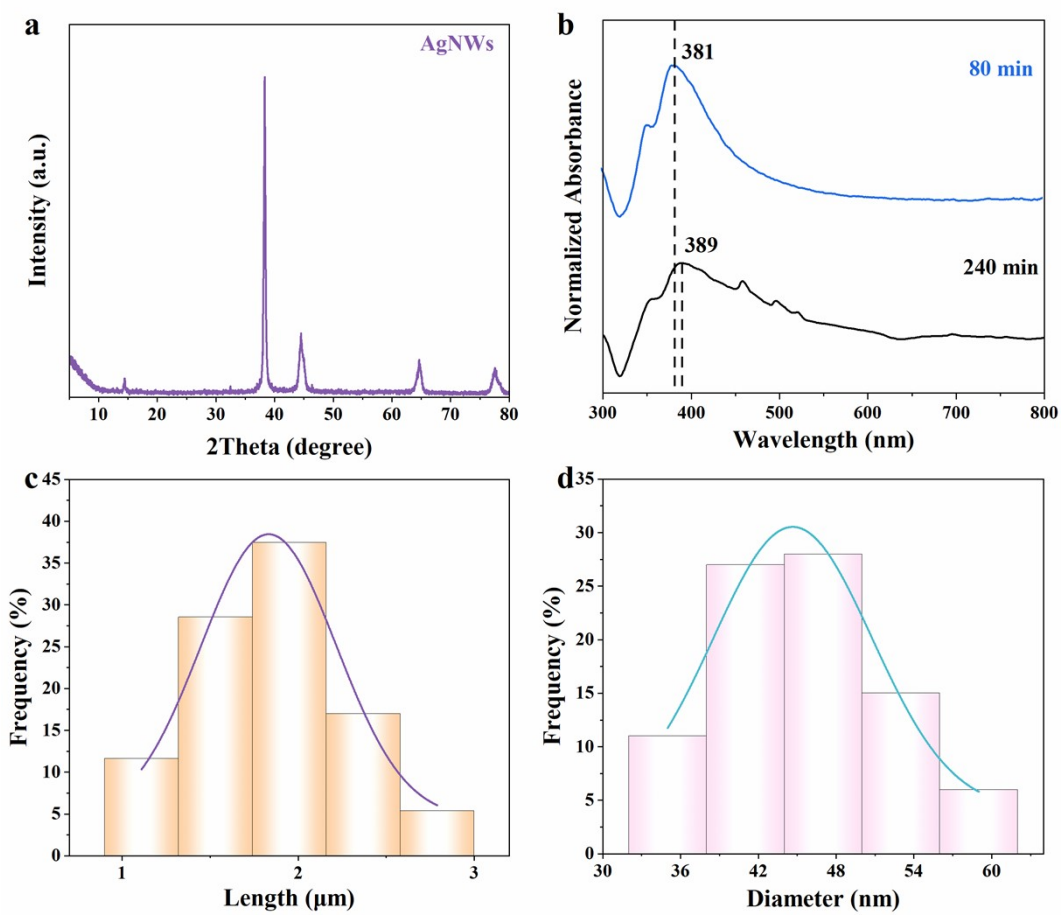

Fig. S5. (a) XRD patterns of AgNWs; (b) UV–vis spectra of AgNWs prepared with different reaction times; (c and d) Histograms of length and diameter that display the AgNWs distribution, respectively.

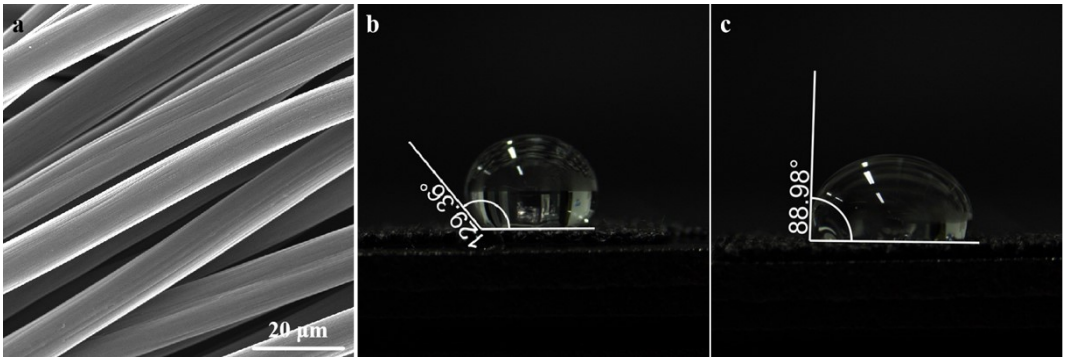

Fig. S6. (a) SEM images of pure carbon cloth; (b and c) Water contact angle of carbon cloth and carbon cloth after treatment.

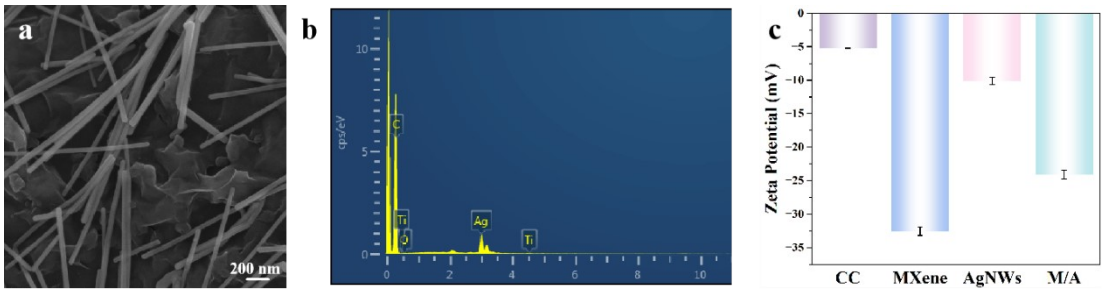

Fig. S7. (a) SEM images of MXene/AgNWs; (b) EDS of the CMA; (c) Zeta-potential of CC, MXene, AgNWs and MXene/AgNWs composites.

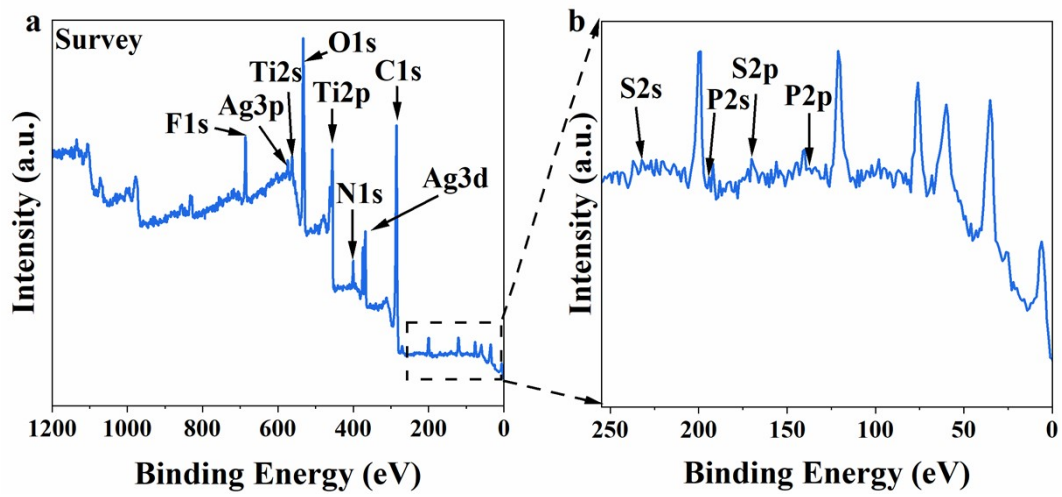

Fig. S8. XPS spectra of CMA-Apt: (a) survey spectrum, and (b) Binding Energy of 0~250 eV.

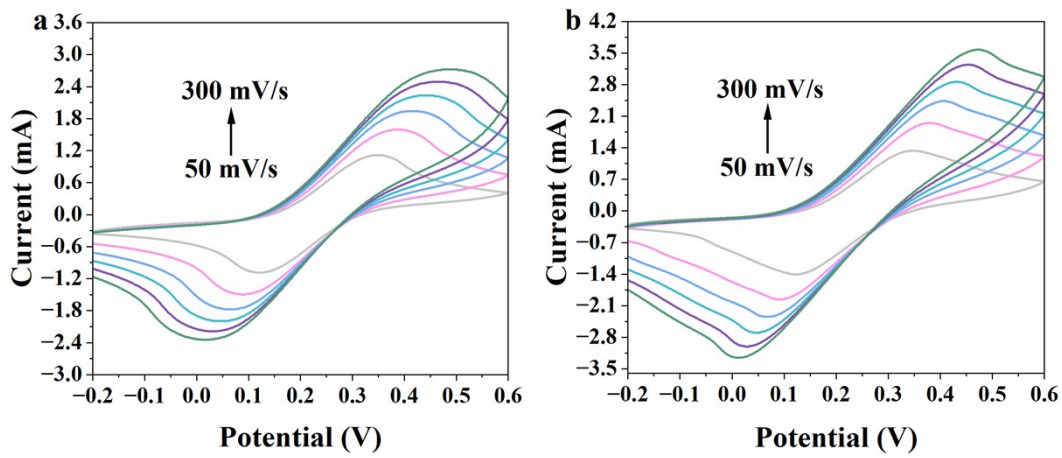

Fig. S9. CV curves of (a) CC film-based electrode and (b) CM film-based electrode at different scan rates from 50 mV/s to 300 mV/s. The system of CV contains 10 mM $K_3[Fe(CN)_6]$ and 0.1 M KCl.

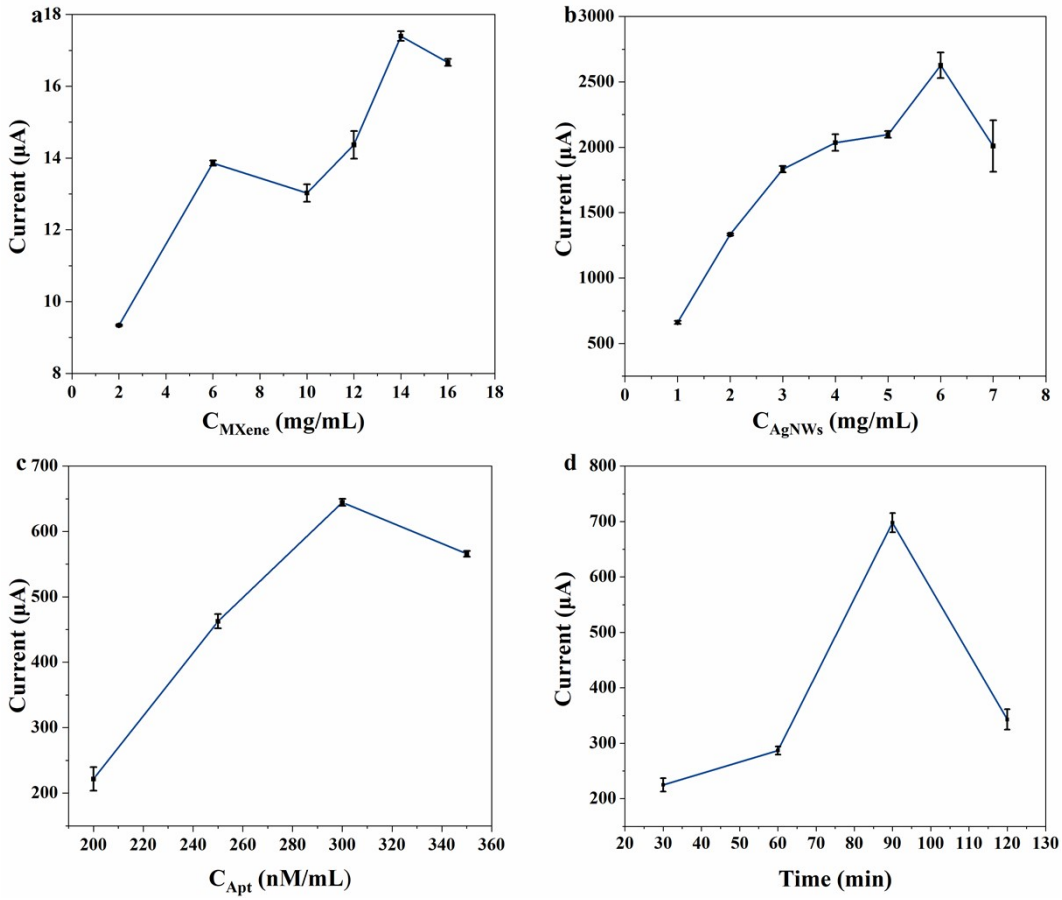

Fig. S10. The effect of different parameters on the biosensing performance of the as-prepared biosensor by DPV responses. (a) The concentrations of MXene. (b) The concentrations of AgNWs. (c) The concentrations of aptamer, and (d) The incubation time of aptamer.

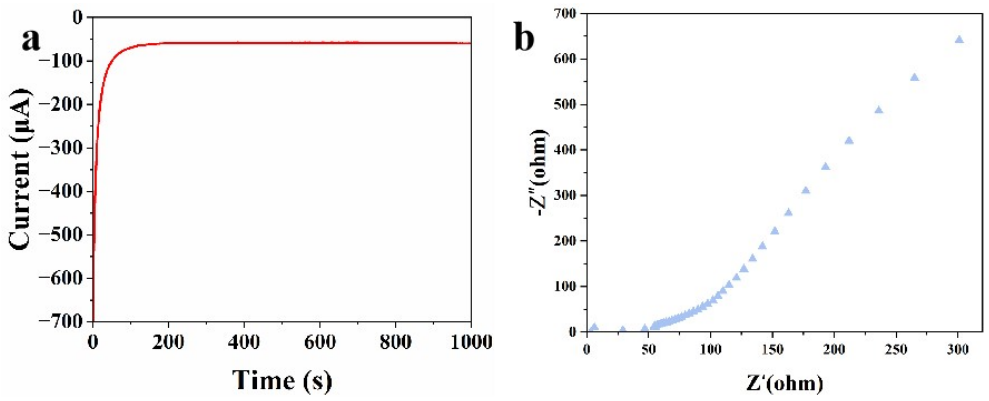

Fig. S11. (a) Chronoamperometric stability of the response to 2×10^5 CFU/mL of *S. aureu*s for the CMA film-based biosensor. The current signal increased by 3.5 % from 400 s to 1000 s, confirming the excellent electrochemical stability of the prepared biosensor during its detection process; (b) EIS measurements of CMA film electrodes after 10,000 bending cycles (r = 2 nm). The resistance of the CMA films did not change significantly after bending cycles, which indicates the recyclability and stability of the prepared material.

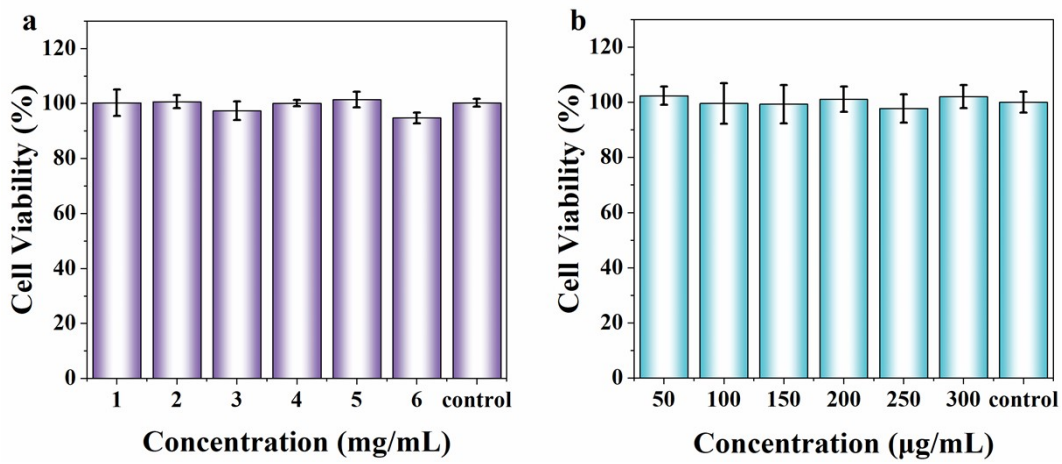

Fig. S12. Cell viability of A549 cells after treatment with different concentrations of MXene/AgNWs for (a) 15 min and (b) 18 h.

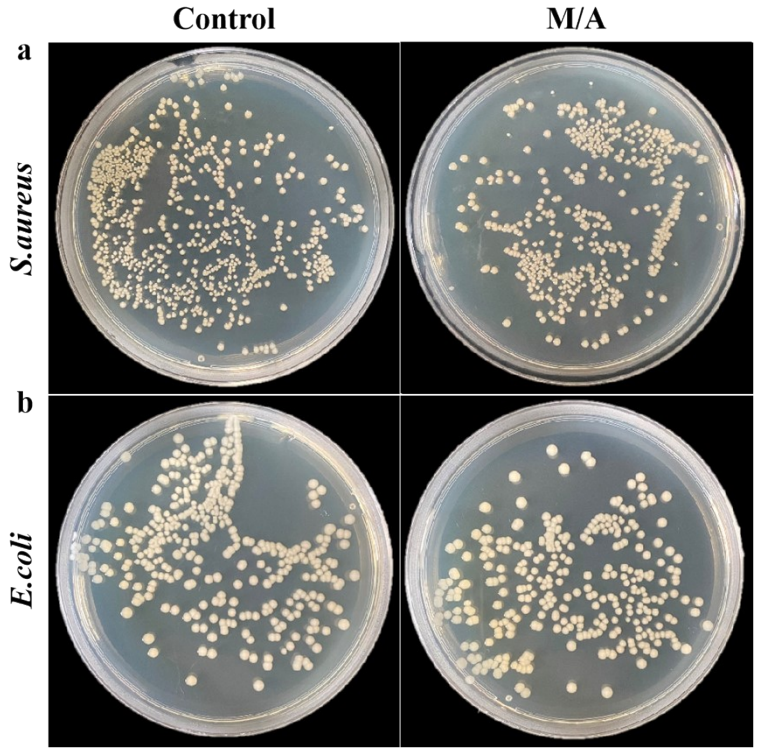

Fig. S13. Photographs of colonies formed by (a) *S. aureus* and (b) *E. coli* after being treated with MXene/AgNWs for 15 minutes. Left: control group; right: experimental group.

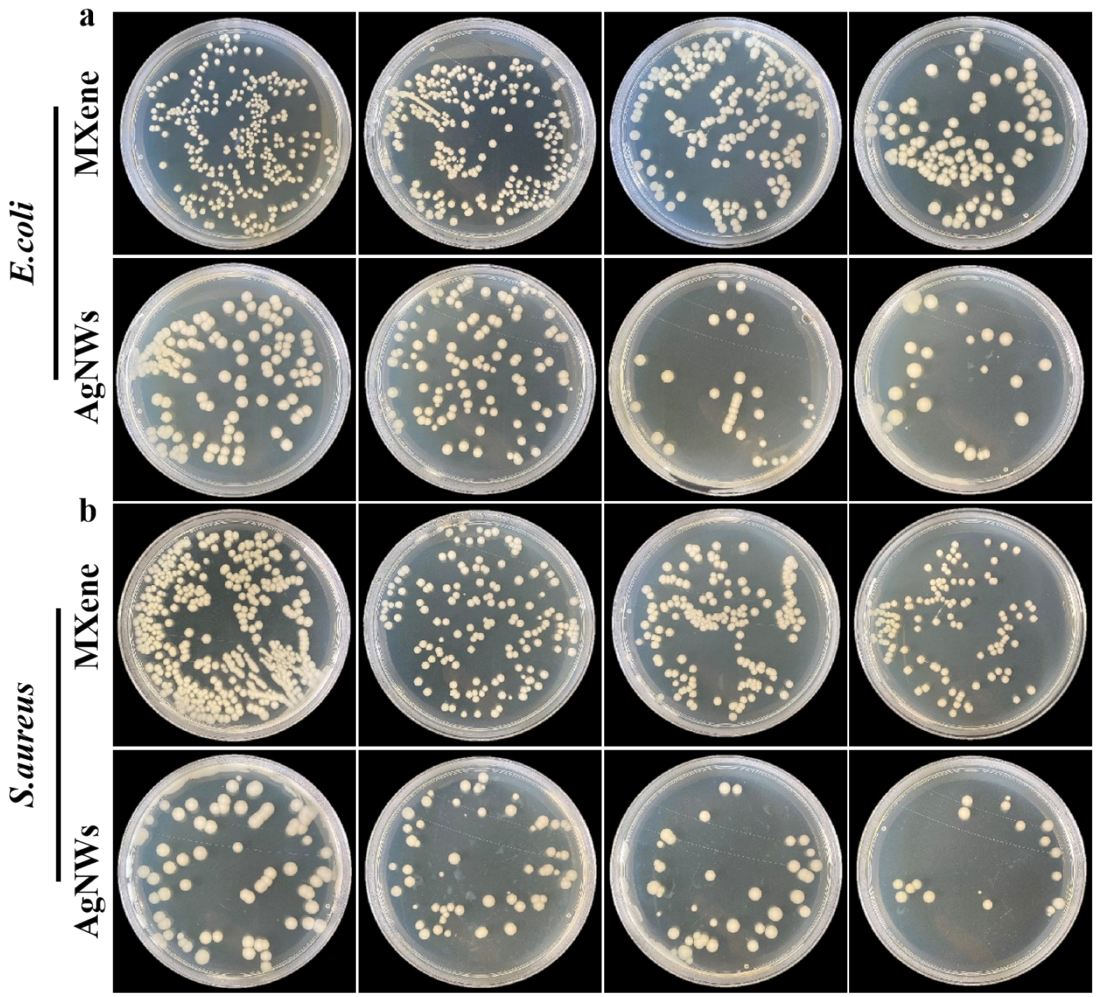

Fig. S14. Photographs of colonies formed by (a) *E. coli* and (b) *S. aureus* after 12 h treatment with MXene and AgNWs, respectively. Top: after treatment with MXene at concentrations of 33, 50, 67, and 83 μg/mL; bottom: after treatment with AgNWs at concentrations of 100, 150, 200, and 250 μg/mL.

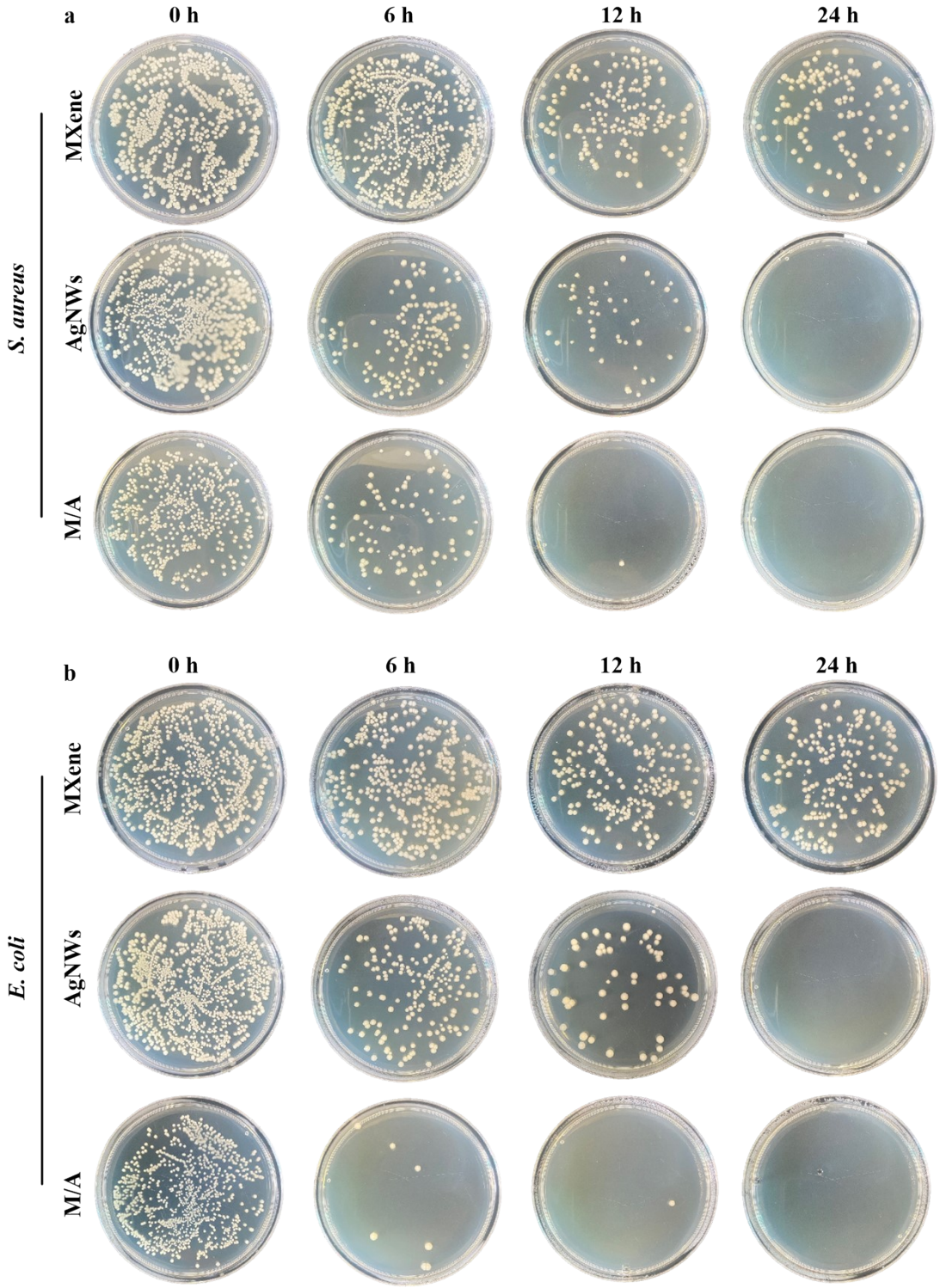

Fig. S15. 24 h bactericidal profiles of MXene, AgNWs and MXene/AgNWs against (a) *S. aureus* and (b) *E. coli*, respectively.

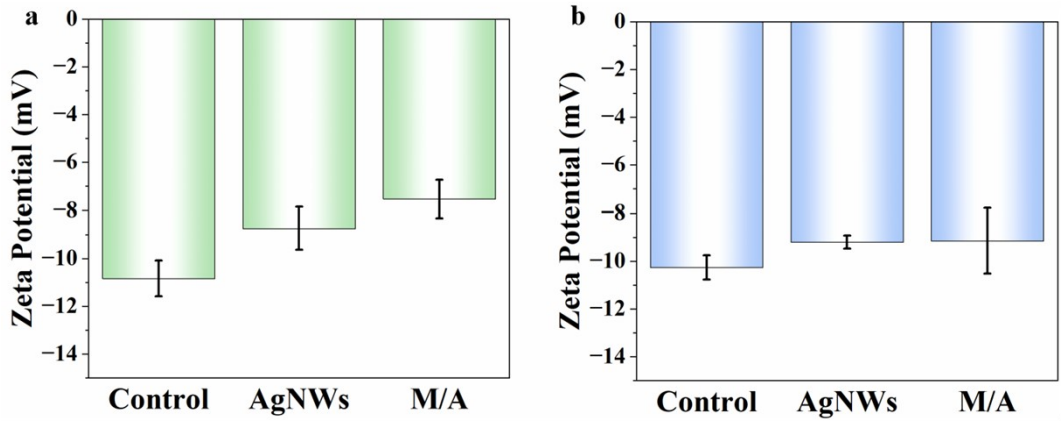

Fig. S16. Zeta potential of (a) *S. aureus* and (b) *E. coli* treated with different materials.

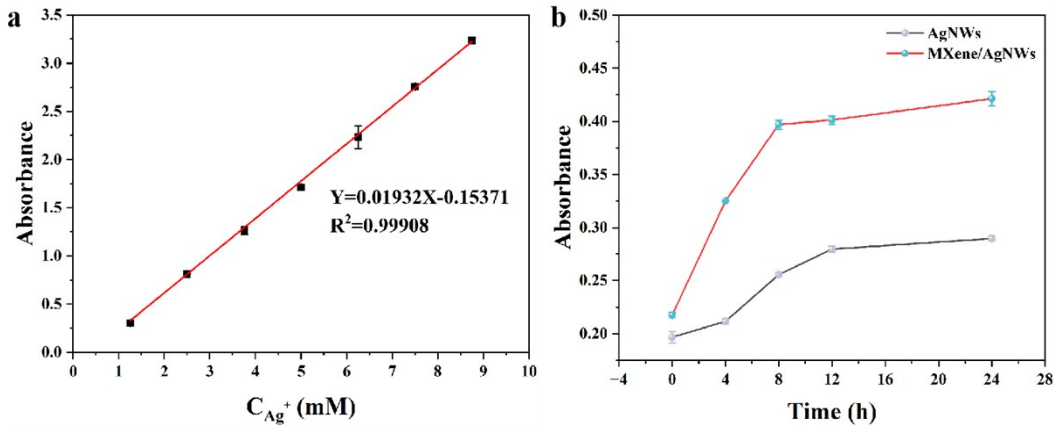

Fig. S17. (a) Standard curve of Ag^+ concentration versus absorbance between 1 mM to 9 mM. (b) Ag^+ concentration of AgNWs and MXene/AgNWs as a function of time from 0 to 24 h.

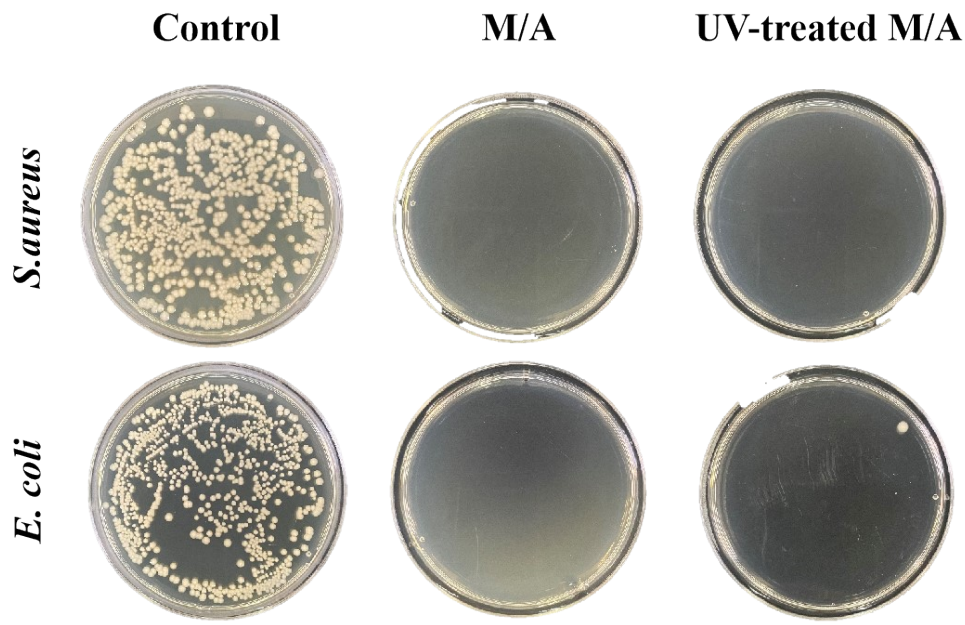

Fig. S18. Photographs of colonies formed by *S. aureus* and *E. coli* after 12 hours of treatment with MXene/AgNWs and UV irradiation for 30 min with MXene/AgNWs. The antimicrobial properties of the composites against Staphylococcus aureus and Escherichia coli did not change significantly after 30 min of UV irradiation, which proved that the materials had good reproducibility.

Table S1. Comparison of the detection performance for the *S. aureus* with other reported work.

Materials	Method	Linear range (CFU/mL)	LOD (CFU/mL)	Ref.
IgY-Cu-PDA	Immunoassay	10 - 2.5×10^4	3	[1]
CBD-HRP-$Cu_3(PO_4)_2$	ELISA	10 - 10^6	6	[2]
VAN-HRP-$CaHPO_4$	ELISA	10^2 - 10^7	4.3	[3]
AMP-MOGs (Fe)	Chemiluminescence	10^2 - 10^7	31	[4]
Au@PtNEs	Colorimetry	5.0×10 – 5.0×10^5	40	[5]
Au NPs@NTP	SERS	8.0 – 8.0×10^6	1.5	[6]
UCNPs-mSiO_2	Fluorescence	6.3×10 – 6.3×10^6	25	[7]
HCAA@UiO-66	Fluorescence	1.05×10^3 - 1.05×10^7	12	[8]
WS_2 QDs	Fluorescence	10^3 - 10^7	850	[9]
HRP-UCNPs-cDNA	Fluorescence	5.6×10 – 5.6×10^6	22	[10]
1L-WS_2	Photoluminescence	10^2 - 10^7	2	[11]
MWCNTs-AuPdPt	Electrochemical	1.1×10^2 - 1.1×10^7	39	[12]
Carbon cloth/MXene/AgNWs	Electrochemical	2.0×10^2 – 2.0×10^7	0.35	This work

Table S2. Comparison of antimicrobial properties of MXene/AgNWs with other reported work.

Materials	*S. aureus* antimicrobial rate (%)	*E. coli* antimicrobial rate (%)	Ref.
$Ti_3C_2T_x$-Au NPs	-	91.95	13
Ti_3C_2-Au CNC + NIR	97.12	88.74	14
carbon fiber/ $Ti_3C_2T_x$ + NIR	60.2	76.3	15
PLA/nano-ZnO/additives non-woven fabrics	98.13	98.52	16
MXene/AgNWs	99.8	99.5	This work

References

1. J. Wang, L. Tan, W. Bi, H. Shen, D. Li, Z. Yu and N. Gan, *Food Chemistry*, 2022, **378**, 132093.
2. W. Yin, L. Zhu, H. Xu, Q. Tang, Y. Ma, S.-H. Chou and J. He, *Sensors and Actuators B: Chemical*, 2022, **366**, 132005.
3. M. Zhao, X. Yao, J. Li, H. Hu, J. Ren, J. Xu, J. Wang and D. Zhang, *Biosensors and Bioelectronics*, 2023, **230**, 115264.
4. Y. Zhang, G. Cui, N. Qin, X. Yu, H. Zhang, X. Jia, X. Li, X. Zhang and X. Hun, *Chemical Communications*, 2020, **56**, 3421-3424.
5. B. Gao, Y. Ding, Z. Cai, S. Wu, J. Wang, N. Ling, Q. Ye, M. Chen, Y. Zhang, X. Wei, Y. Ye and Q. Wu, *Microchim. Acta*, 2024, **191**, 438.
6. A. Zhu, Z. Wang, L. Peng, Y. Xu, T. Jiao, Q. Ouyang and Q. Chen, *Sensors and Actuators B: Chemical*, 2025, **425**, 136977.
7. Q. Ouyang, M. Zhang, Y. Yang, Z.-u. Din and Q. Chen, *Food Control*, 2023, **145**, 109444.
8. J. Qiao, X. Chen, X. Xu, B. Fan, Y.-S. Guan, H. Yang and Q. Li, *Journal of Materials Chemistry B*, 2023, **11**, 8519-8527.
9. A. K. Mia, A. Bora, M. T. Hossain, S. Sinha and P. K. Giri, *Journal of Materials Chemistry B*, 2023, **11**, 10206-10217.
10. Q. Ouyang, L. Wang, W. Ahmad, Y. Yang and Q. Chen, *Journal of Agricultural and Food Chemistry*, 2021, **69**, 9947-9956.
11. A. K. Mia, S. Sinha and P. K. Giri, *Sensors and Actuators Reports*, 2024, **8**, 100214.
12. E. Han, Y. Zhang, J. Cai and X. Zhang, *Journal*, 2021, **12**.
13. L. Jiang, Z. Yu, W. Zhao, Z. Yang, Y. Peng, Y. Zhou, X. Lin and S. Jin, *Anal. Chem.*, 2023, **95**, 1721-1730.
14. Z. Yu, L. Jiang, R. Liu, W. Zhao, Z. Yang, J. Zhang and S. Jin, *Chemical Engineering Journal*, 2021, **426**, 131914.
15. Y. Lian, D. Lan, X. Jiang, L. Wang, S. Yan, Q. Dong, Y. Jiang, J. Gu, Z. Gao and G. Wu, *Journal of*

Colloid and Interface Science, 2024, **676**, 217-226.

16. R. Zhang, L. Tang, X. Ji, Y. Su, N. Xu, Y. Feng and L. Pan, *International Journal of Biological Macromolecules*, 2024, **269**, 132188.